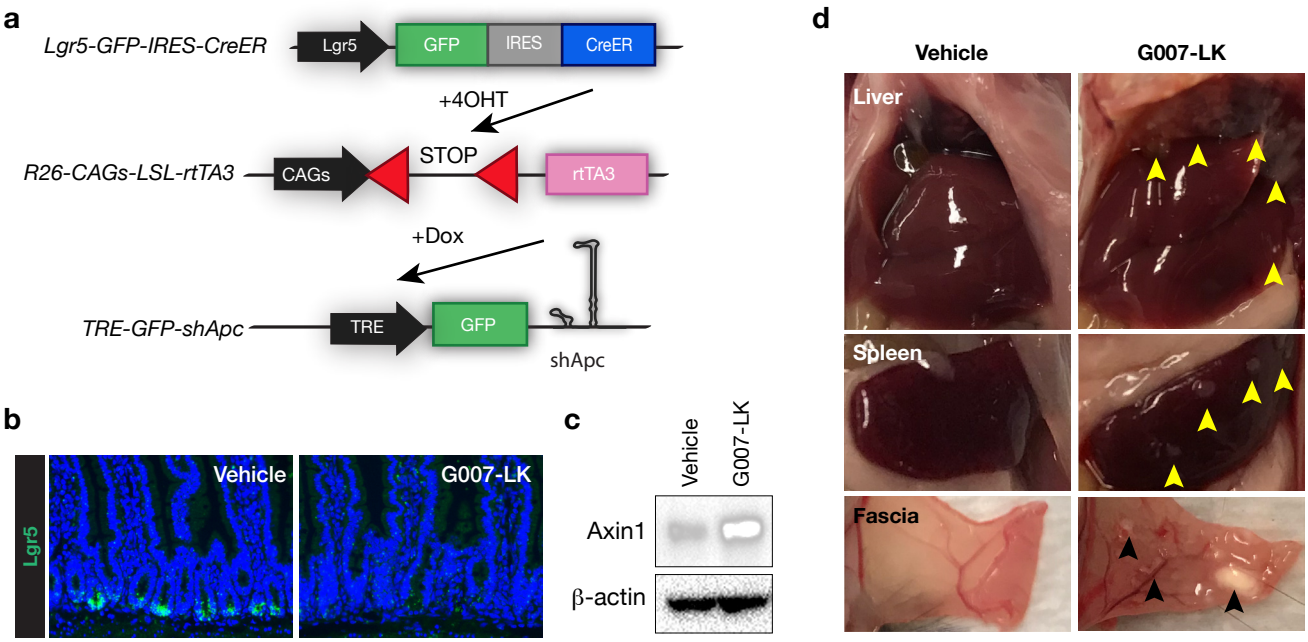

Supplementary Figure 1. G007-LK treatment drives WNT suppression *in vivo*, but is associated with damage to peritoneal organs.
a. Schematic depiction of the alleles used to generate mosaic shRNA knockdown originating in the stem cells of the intestine. **b**. *In situ* hybridization for Lgr5 transcript in small intestinal sections from *Apc*^{Min} mice treated either with vehicle or G007-LK (30mg/kg) for one week. **c**. Western blot of whole tissue lysates extracted from the intestinal villi of mice treated with Vehicle or G007-LK for one week, confirming Axin1 stabilization. Tissue collected ~20hrs after final drug dose. **d**. Images of adhesions visible on the liver, spleen, and fascia in mice after 1 week of G007-LK treatment.

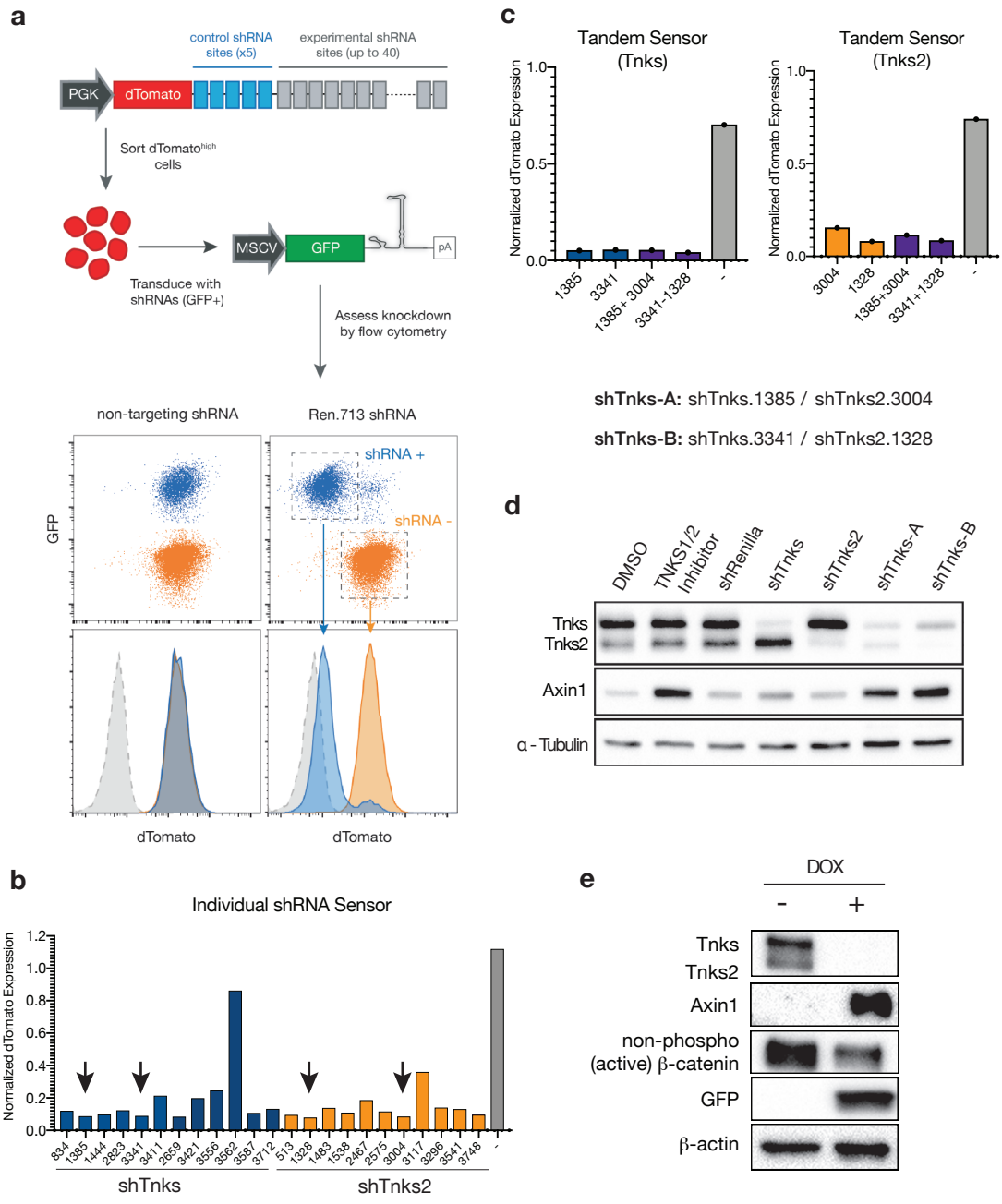

Supplementary Figure 2. Strategy to identify potent shRNAs targeting Tnks and Tnks2.
a. Schematic of the dTomato sensor construct followed shRNA target (sense) sequences in the 3'UTR. **b.** Bar graph showing background subtracted, normalized dTomato expression following expression of either Tnks or Tnks2 shRNAs, as indicated. **c.** Bar graphs showing normalized dTomato expression following expression of either individual Tnks and Tnks2 shRNAs, or tandem construct. The tandem shRNA cassettes enable equivalent knockdown to the single shRNAs. Below, is the key for referencing the independent tandem constructs. **d.** Western blot from NIH3T3 whole cell lysates transduced with shRNAs, as indicated, or treated with TNKS inhibitor (XAV939). **e.** Western blot on whole cell lysates from intestinal villi of *CAGs-rtTA3/TG-shTnks-A* mice treated with or without doxycycline (200mg/kg, in chow) for 2 weeks shows Tnks1/2 silencing, Axin1 stabilization, and decreased active β-catenin.

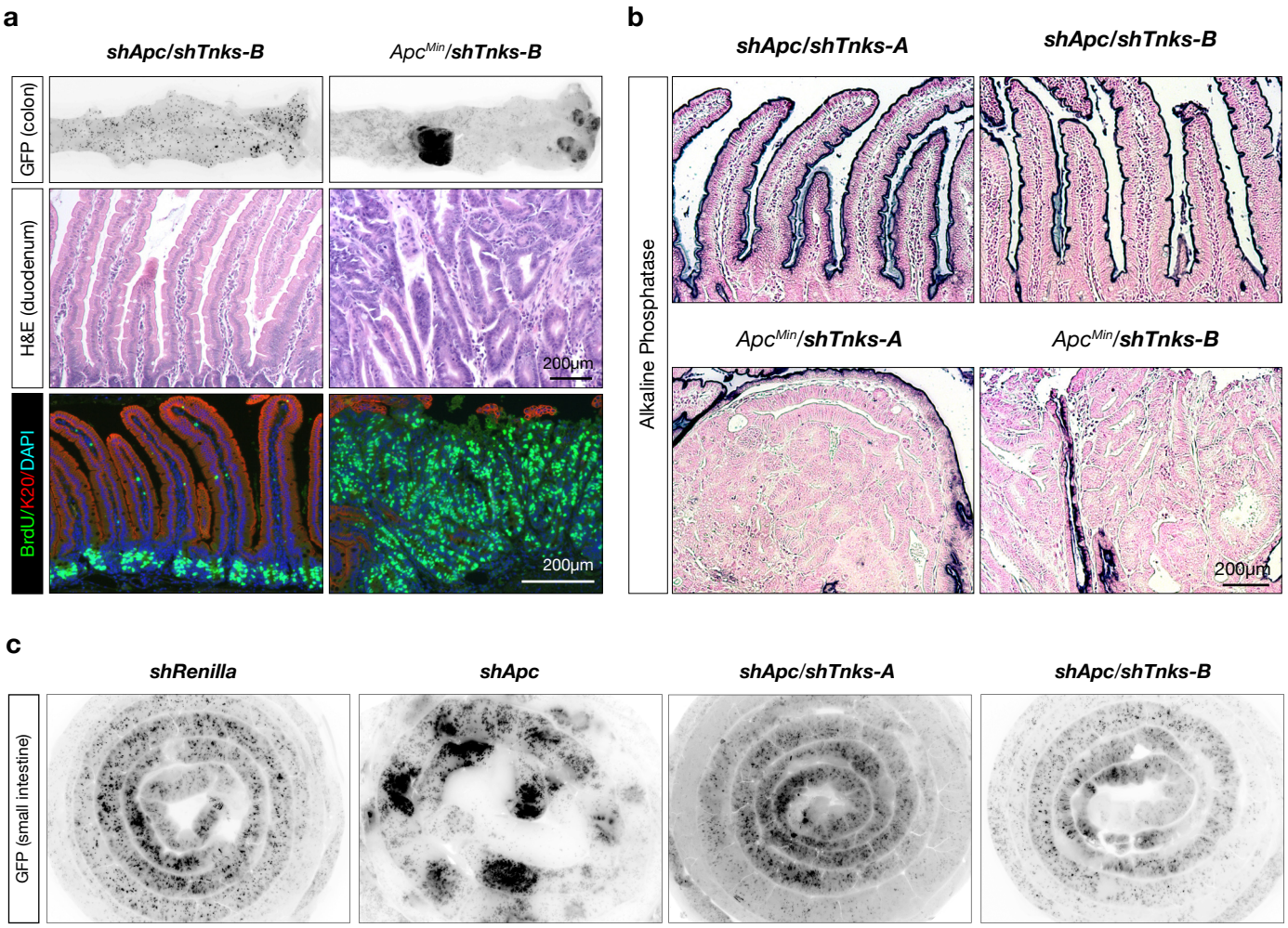

Supplementary Figure 3. Tnks1/2 silencing blocks shApc but not Apc^{Min} tumor growth.
a. Epifluorescent images from representative colon images of shApc/shTnks1/2-1385-3004, Apc^{Min}/shTnks1/2-1385-3004 mice sacrificed at the experimental endpoint. Immunohistochemical and immunofluorescent stains of representative small intestinal sections. **b.** Alkaline phosphatase staining of small intestinal sections from shApc/shTnks1/2 and Apc^{Min}/shTnks1/2 mice for both independent shRNA sets. **c**. Epifluorescent images of whole mount small intestine of *shRenilla*, *shApc*, *shApc/shTnks1/2-3341-1328*, and *shApc/shTnks1/2-1385-3004* at experimental endpoint. Black signal represents GFP expression.

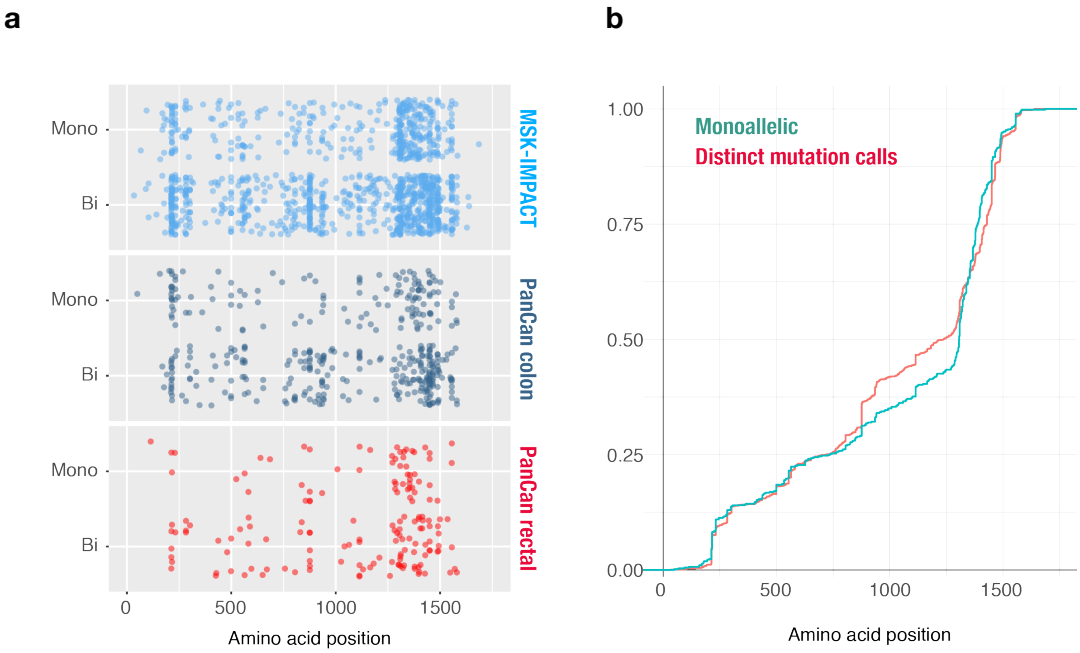

Supplementary Figure 4. Position of nonsense Apc mutations in human CRCs
a. Amino acid position of nonsense APC mutations in three independent CRC datasets, segregated by whether the tumors show two distinct mutations (Bi) or a single nonsense allele (Mono). The majority of mutations in Apc lie in the mutation cluster region (MCR), between AA 1250 and 1580, and tumors that contain a single identifiable APC allele are further biased toward the MCR. **b.** Cumulative frequency plot showing the occurrance of nonsense mutations in APC in tumors with single identifiable APC mutations (Monoallelic), and those with two distinct alleles. This plot more clearly Illustrates the higher frequency of MCR truncations in tumors with a single APC mutation (either homozygous or mutant/LOH).

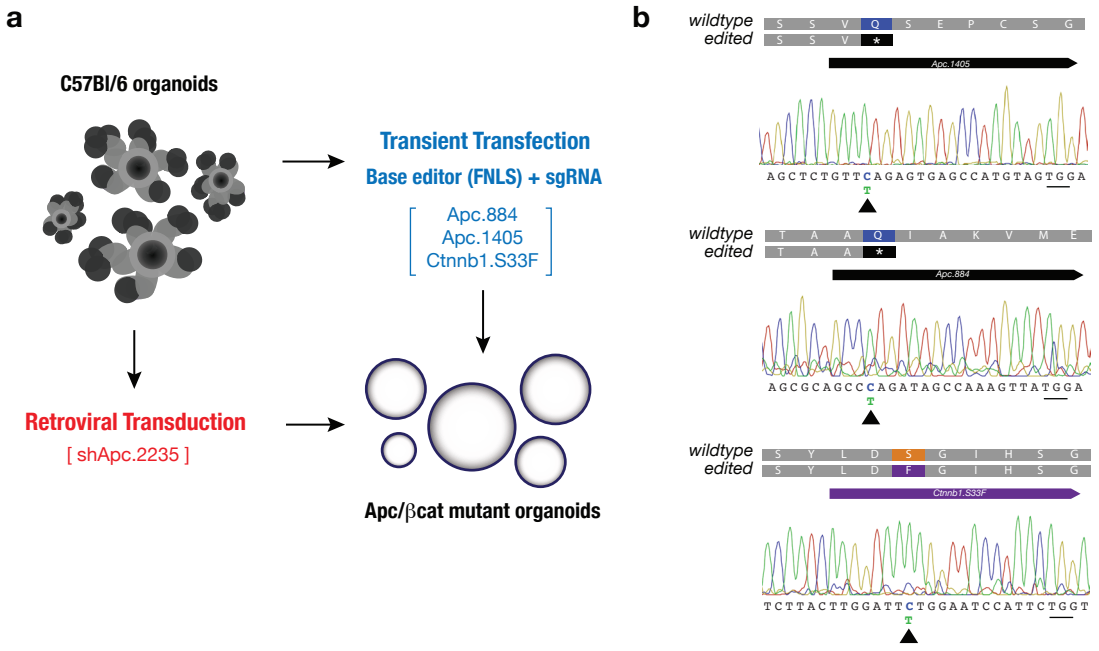

Supplementary Figure 5. Generation of mutant organoids by base editing and shRNA knockdown
a. Schematic depiction of strategy used to generate Apc mutant organoids by lipofectamine-based transfection or retroviral transduction. **b.** Sanger sequencing chromatograms showing each mutation generated by base editing alongside predicted amino acid change.

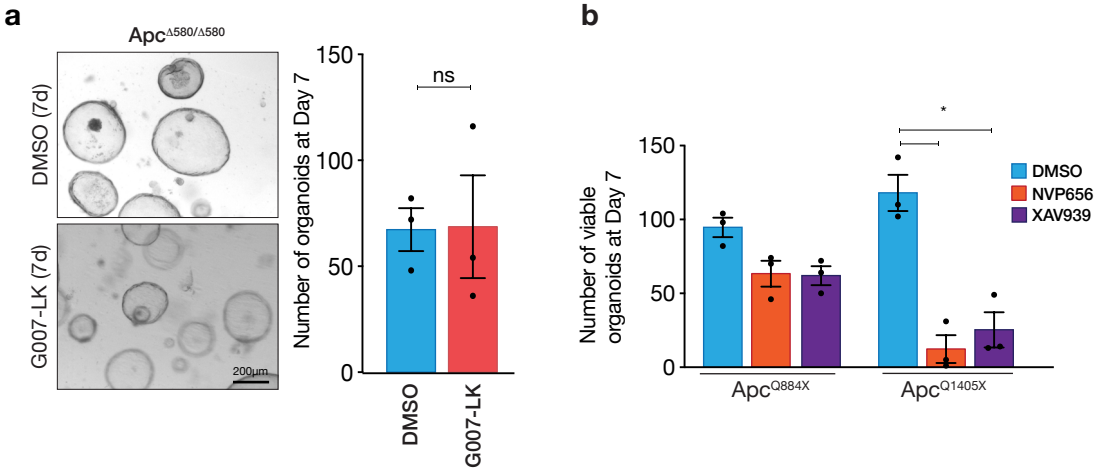

Supplementary Figure 6. Apc$^{\Delta 580}$ organoids do not respond to G007-LK, but ApcQ1405X organoids respond to multiple TNKS inhibitors
a. Brightfield images and quantification of viable *Apc$^{\Delta 580/\Delta 580}$* organoids after treatment with DMSO or G007-LK(1μM) for 7 days. **b.** Quantitation of viable organoids (genotypes as indicated) after 7 days of DMSO, NVP656 (1μM) , or XAV939 (1μM) treatment (n=3-4, error bars = s.e.m, * p value ≤ .05, unpaired t-test with Welch's correction). All organoids were passaged once at day 3.

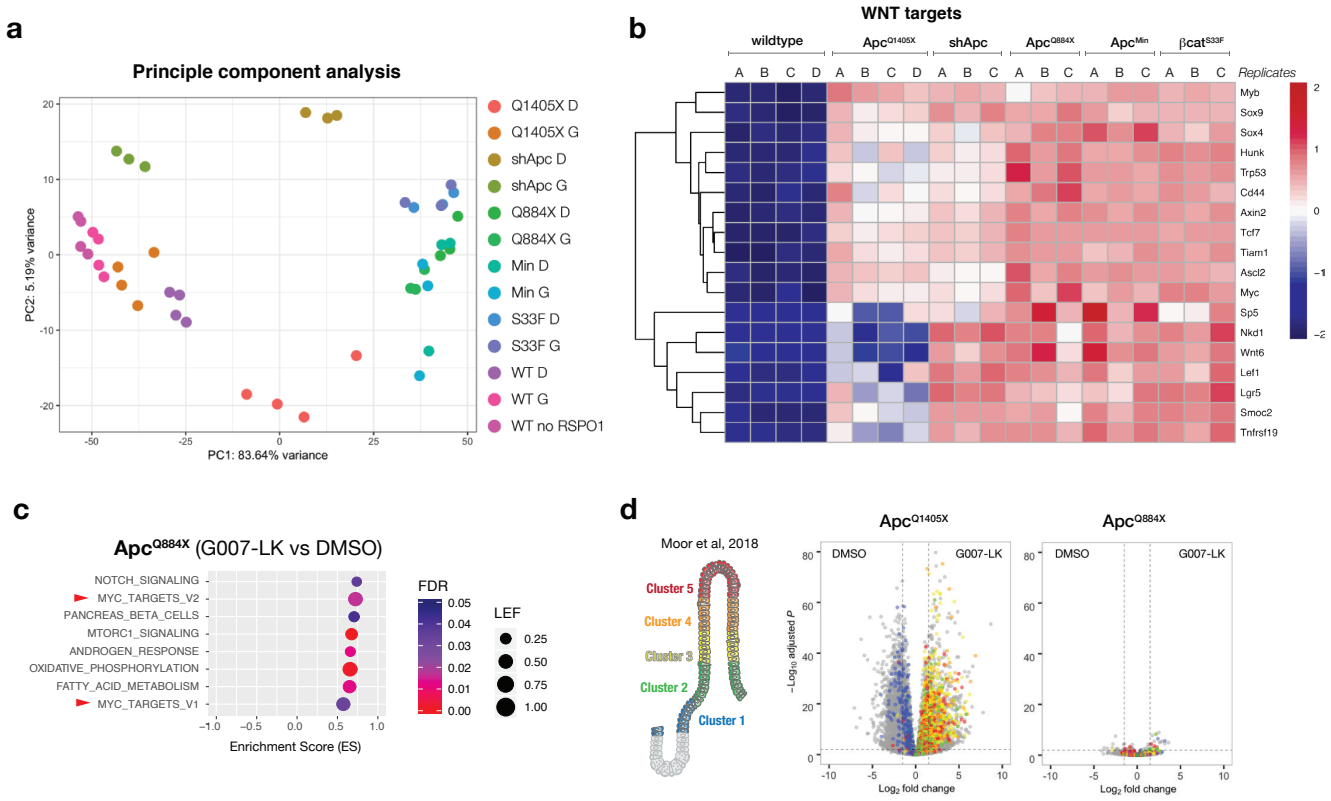

Supplementary Figure 7. Genomic analysis of G007-LK treated organoids reveals normal intestinal differentiation signature.
a. PCA plot showing clustering of wildtype, Apc and βcat^{S33F} mutants based on transcriptome data. Each principle component comprised a maximum of 500 genes. G=G007-LK, D=DMSO. **b**. Heatmap representing relative gene expression in wildtype, Apc and βcat^{S33F} organoids cultured in DMSO (D) or G007-LK (G) for 3 days. Shown are 1472 genes with a log2FC >2 and adj p-value <0.01 in G007-LK-treated WT organoids, compared to DMSO controls. **c**. Summary plot of GSEA results, including 10 significantly positively enriched gene sets in G007-LK treated Apc^{Q1405X} and Apc^{Q884X} organoids. No genesets were significantly negatively enriched. Leading Edge Fraction (LEF) is the fraction of genes in the geneset included in the leading edge of the GSEA plot. **d.** Schematic depiction of the cell populations identified by gene signatures in Moor *et al*. 2018. Adjacent color-coded volcano plots of G007-LK treated Apc^{Q1405X} and Apc^{Q884X} organoids highlight genes included in these signatures. Those genes upregulated following G007-LK treatment appear to the right of the volcano plot.

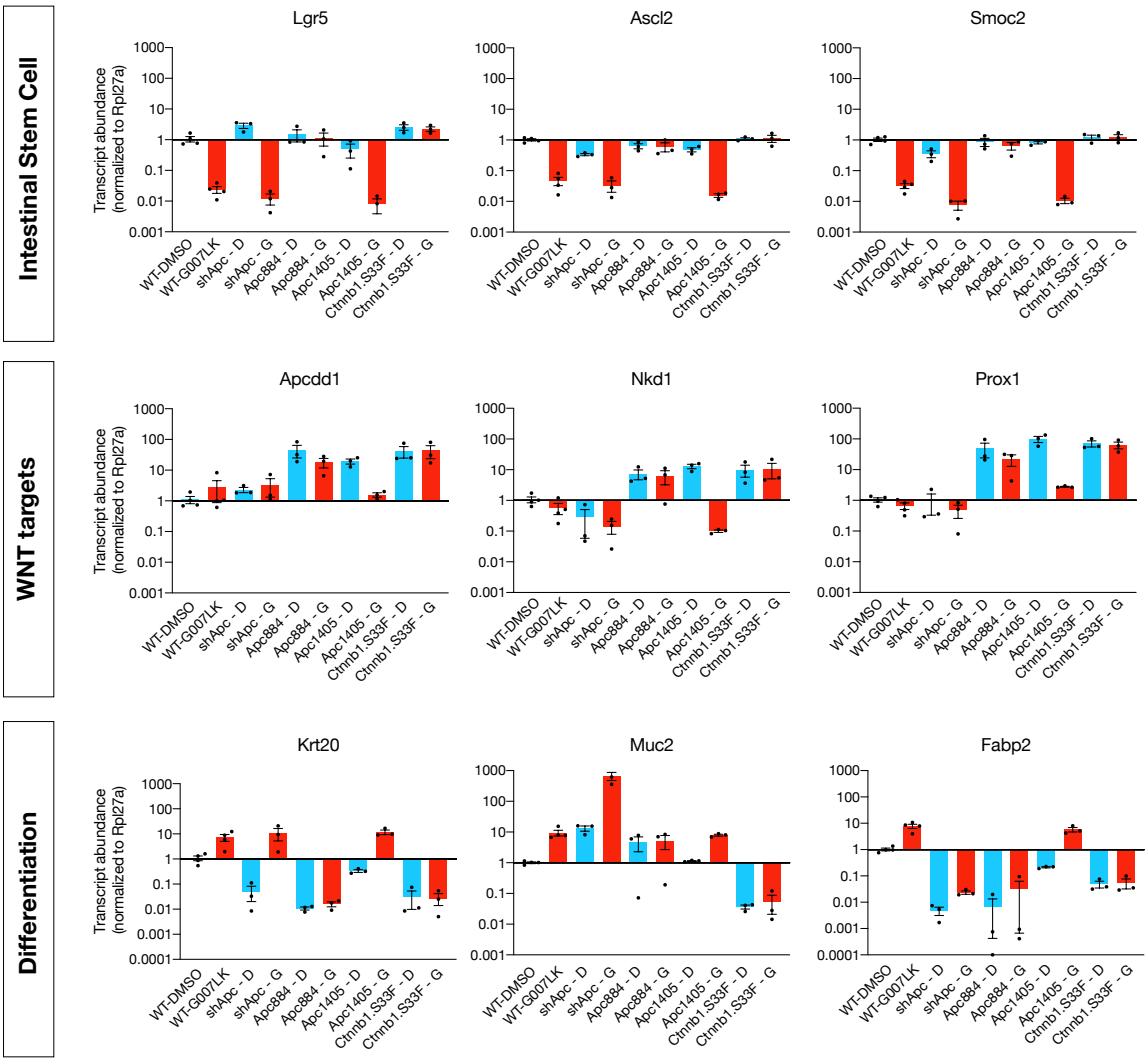

Supplementary Figure 8. Transcriptional Changes in stem cell, differentiation, and WNT targets genes.
Quantitative RT-PCR results for intestinal stem cell markers Lgr5, Ascl2, Smoc2 (top), WNT target genes Apcdd1, Nkd1, Prox1 (middle), and differentiation markers Krt20, Muc2, Fabp2 (bottom). Data represent n=3-4, mean +/- SEM.

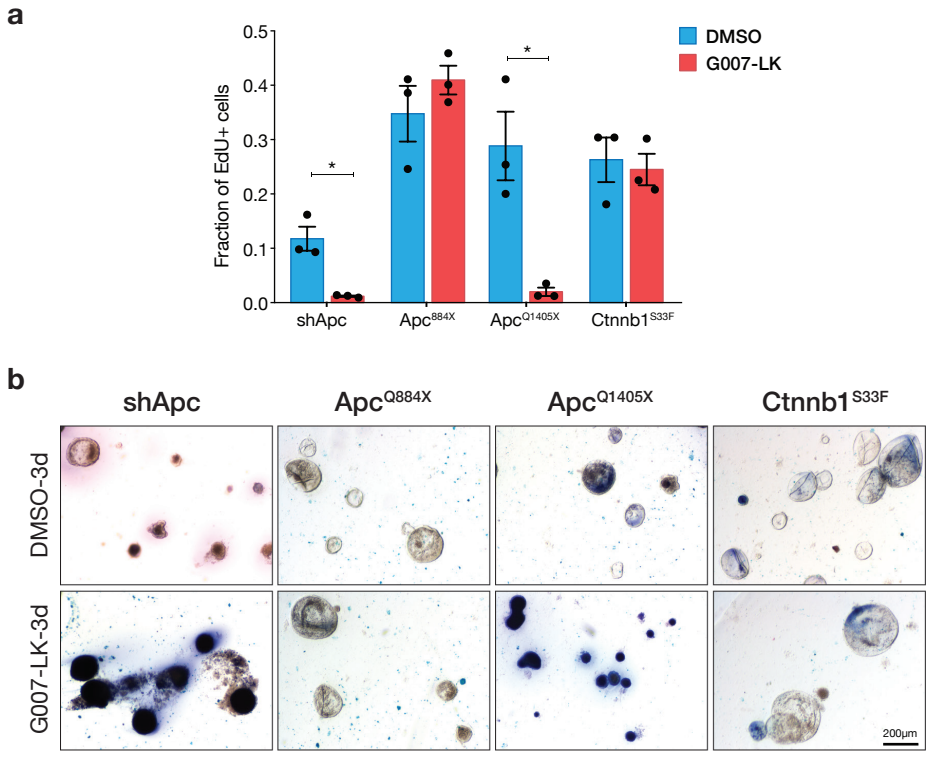

Supplementary Figure 9. Only late Apc truncation organoids arrest and differentiate in response to Tankyrase inhibition.
a. Quantification of EdU staining in Apc or β-catenin mutant organoids after 3 days of treatment with DMSO or G007-LK, then pulsed with EdU for 4 hours. **b.** Brightfield images of wholemount alkaline phosphatase staining of Apc or β-catenin mutant organoids treated with DMSO or G007-LK (1μM) for 3 days. Blue color indicates intestinal alkaline phosphatase activity in the organoids from differentiated enterocytes.

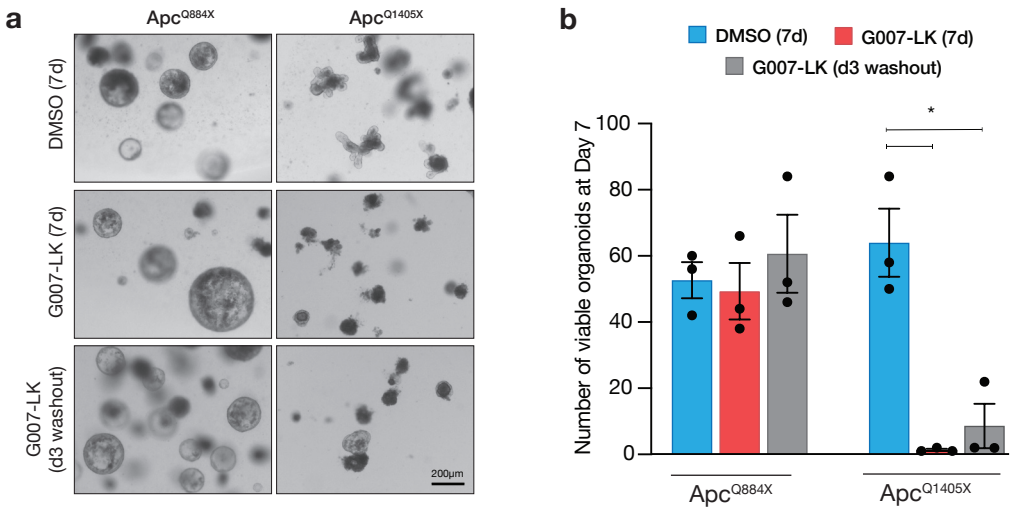

Supplementary Figure 10. Washout of G007-LK after 3 days does not dramatically improve organoid survival
a. Brightfield images of Apc-mutant organoids treated with DMSO or G007-LK(1μM) for 3 or 7 days, or treated with G007-LK for 3 days and then DMSO for 4 days (d3 washout). **b.** Bar graph quantifying the number of viable Apc-mutant organoids at Day 7. Apc^{Q1405X} organoids did not show significant recovery following washout of the drug at day 3 (n=3, error bars = s.e.m, * $p < 0.05$, unpaired t-test with Welch's correction).

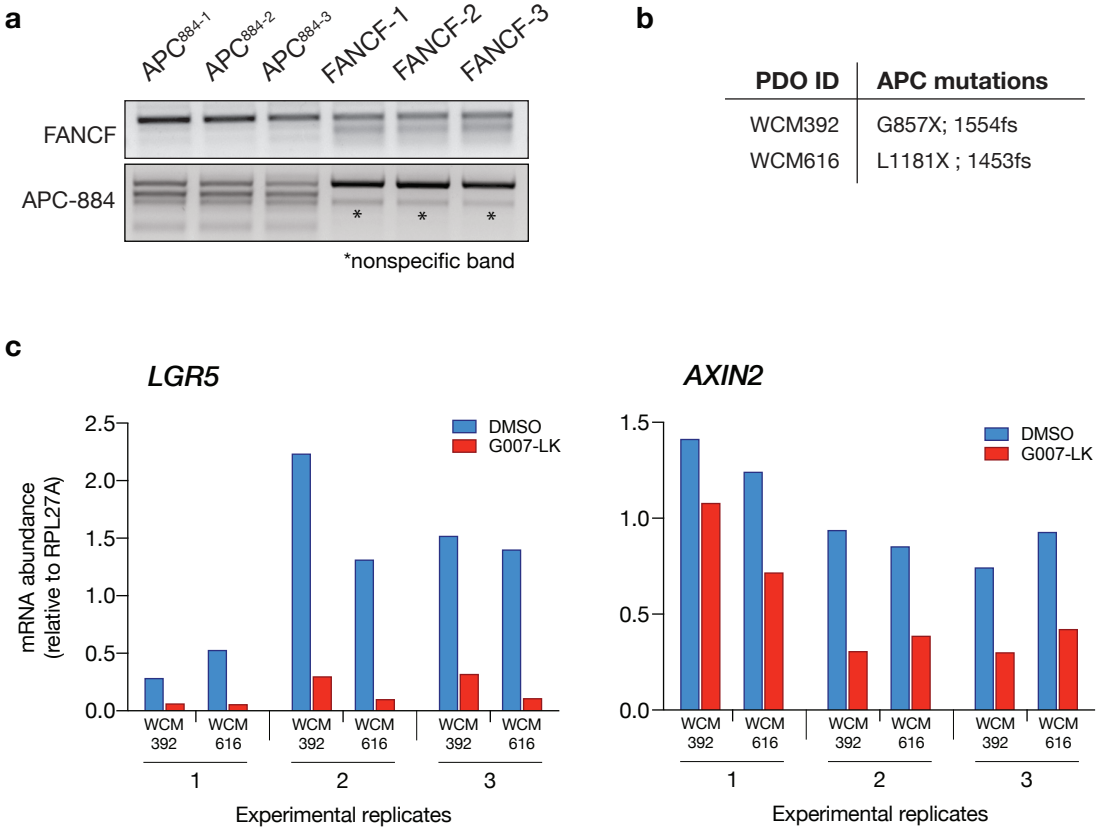

Supplementary Figure 11. Human organoids with a late truncation in APC suppress WNT targets in response to G007-LK.
a. T7 endonuclease assay of the FANCF or APC target loci in DLD1-Cas9 cells expressing either the APC-884 or FANCF guide, after 7 days of selection in blasticidin. Only cells expressing their respective guide show cleavage in target loci. **b**. APC mutations identified in patient-derived human colorectal cancer organoid (PDO) samples. Mutations called from whole exome sequencing (WES) (Pauli et al, *Cancer Discovery*, 2017). **c**. Bar graphs showing quantitative RT-PCR results from individual experimental replicates of G007-LK treated patient derived organoids with late APC truncations. Each experiment represents an independent treatment, RNA isolation and qRT-PCR analysis. Absolute values (relative to RPL27A) varied between experiments, but fold change following G007-LK treatment was consistent.

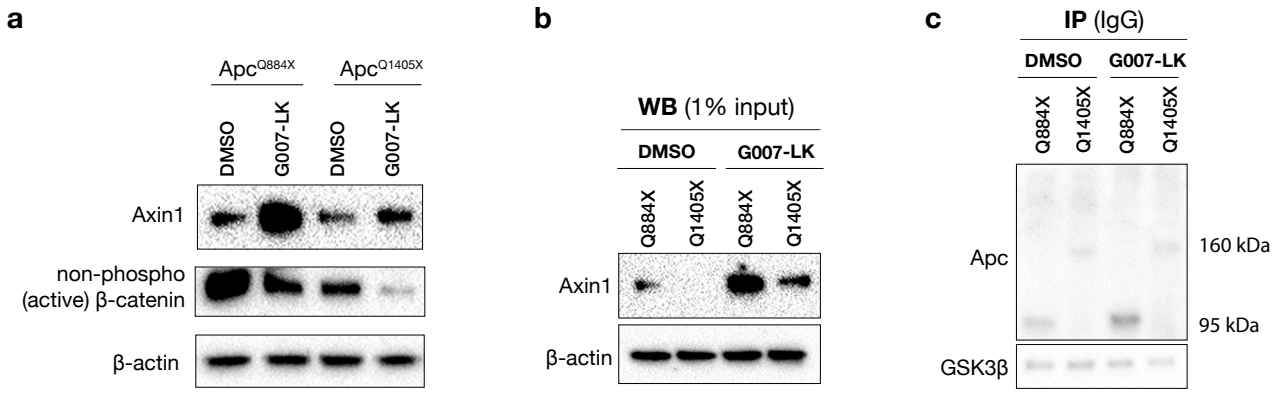

Supplementary Figure 12. Tnks1/2 inhibition increase stability of Axin1-Apc's ability to recruit and phosphorylate β-catenin. **a**. Western Blot from Apc mutant organoids showing Axin1 stabilization after G007-LK (1μM) treatment for 3 days, and decreased non-phosphorylated (active) β-catenin. **b**. Western blot of 1% immunoprecipitation input showing Axin1 stabilization after G007-LK (1μM) treatment for 24 hours. **c.** Western Blot showing IgG control for immunoprecipitation experiments in **Figure 3k**.

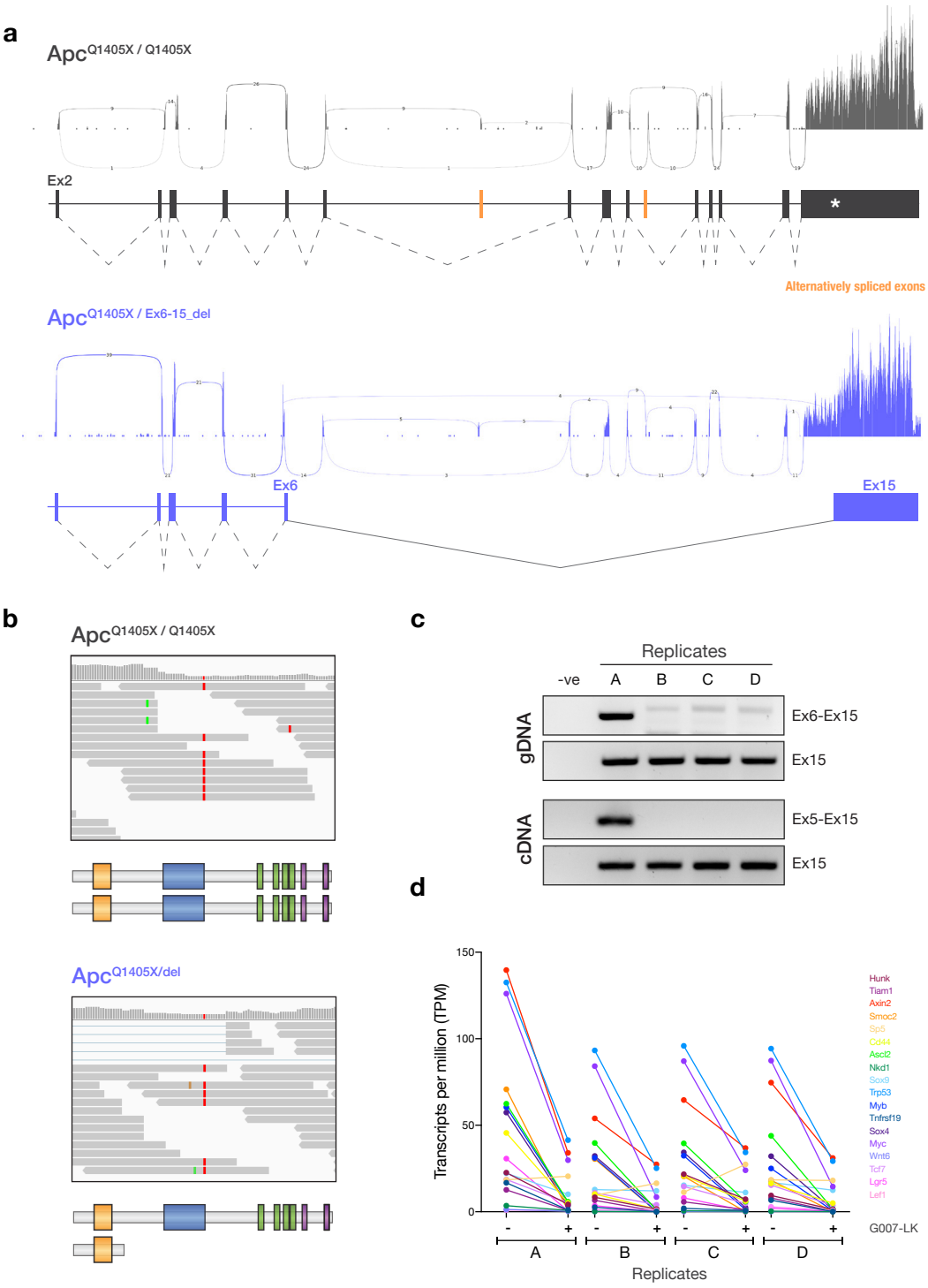

Supplementary Figure 13. Apc^{Q1405X} mutant organoids carrying a single copy of the Q1405X truncation are equally responsive to Tnks1/2 inhibition

a. Sashimi plot of the deletion event between Exon 6 and Exon15 occurring in in Apc^{Q1405X} replicate A (blue). Sashimi plot of replicate B (similar to C & D) is shown above for reference (grey). **b.** Raw RNA sequencing IGV read pile-ups, showing Q1405X mutation (red) and reads spanning the deletion event, with the breakpoint 3' to the editing target site - near the PAM site. Schematic image of the predicted Apc products in biallelic Apc^{Q1405X} organoids (upper), compared to replicate A (lower). **c.** Agarose gel showing amplification of deletion PCR products specifically in replicate A samples. Amplification of the Exon 15 target region is included as a control for genomic DNA and cDNA quality. The large deletion predicted from RNAseq analysis was confirmed in both genomic DNA and cDNA from these samples. **d.** Normalized data from RNA sequencing analyses showing transcript abundance from WNT target genes (listed on the right). Replicate A (containing the heterozygous deletion) shows higher baseline WNT activation, but shows similar transcriptional response to G007-LK treatment, indicating the presence of one mutant allele is sufficient to enable response to TNKS inhibition.

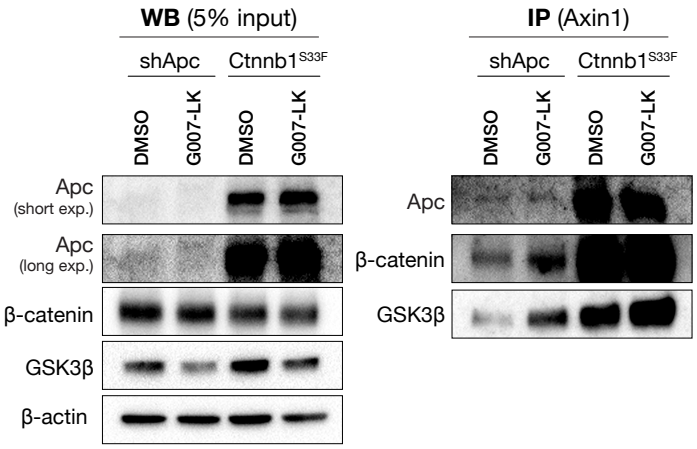

Supplementary Figure 14. Apc protein is detectable in shApc cells in complex with Axin1
Input (left) and Axin1 immunoprecipitation (right) of whole cell lysate from shApc and Ctnnb1^{S33F} mutant cells showing Apc knockdown and detection of Apc protein in complex with Axin1. βcatenin protein association with Axin1 is increased in shApc cells following G007-LK.